

# Measurement of the vector and tensor analyzing powers for $dp$ - elastic scattering at 880 MeV

P.K.Kurilkina<sup>a</sup>, V.P.Ladygina<sup>a</sup>, T.Uesaka<sup>b</sup>, K.Suda<sup>c</sup>, Yu.V.Gurchin<sup>a</sup>, A.Yu.Isupov<sup>a</sup>, K.Itoh<sup>d</sup>, M.Janek<sup>a,e</sup>, J.-T.Karachuk<sup>a,f</sup>, T.Kawabata<sup>b</sup>, A.N.Khrenov<sup>a</sup>, A.S.Kiselev<sup>a</sup>, V.A.Kizka<sup>a</sup>, V.A.Krasnov<sup>a,g</sup>, N.B.Ladygina<sup>a</sup>, A.N.Livanov<sup>a,g</sup>, Y.Maeda<sup>h</sup>, A.I.Malakhov<sup>a</sup>, S.M.Piyadin<sup>a</sup>, S.G.Reznikov<sup>a</sup>, S.Sakaguchi<sup>b</sup>, H.Sakai<sup>i</sup>, Y.Sasamoto<sup>b</sup>, K.Sekiguchi<sup>c</sup>, M.A.Shikhalev<sup>a</sup>, T.A.Vasiliev<sup>a</sup>, H.Witala<sup>j</sup>

<sup>a</sup>VBLHEP-JINR, 141980 Dubna, Moscow region, Russia

<sup>b</sup>Center for Nuclear Study, University of Tokyo, Tokyo 113-0033, Japan

<sup>c</sup>RIKEN Nishina Center, Wako, Saitama 351-0198, Japan

<sup>d</sup>Department of Physics, Saitama University, Saitama, Japan

<sup>e</sup>Physics Department, University of Žilina, 010 26 Žilina, Slovakia

<sup>f</sup>Advanced Research Institute for Electrical Engineering, Bucharest, Romania

<sup>g</sup>Institute for Nuclear Research, Moscow, Russia

<sup>h</sup>Kyushi University, 6-10-1 Hakozaki, Higashi-ku, Fukuoka-shi 812, Japan

<sup>i</sup>University of Tokyo, Bunkyo, Tokyo 113-0033, Japan

<sup>j</sup>Institute of Physics, Jagiellonian University, Kraków, Poland

arXiv:1207.3509v1 [nucl-ex] 15 Jul 2012

---

## Abstract

The vector  $A_y$  and tensor analyzing powers  $A_{yy}$  and  $A_{xx}$  for  $dp$ - elastic scattering were measured at  $T_d^{lab} = 880$  MeV over the c.m. angular range from  $60^\circ$  to  $140^\circ$  at the JINR Nuclotron. The data are compared with predictions of different theoretical models based on the use of nucleon-nucleon forces only. The observed discrepancies of the measured analyzing powers from the calculations require the consideration of additional mechanisms.

PACS: 24.70.+s, 25.10.+s, 21.45.+v

Keywords: Analyzing powers, elastic scattering, polarization

---

## 1. Introduction

The nucleon-deuteron ( $Nd$ ) elastic scattering is the simplest composite-particle scattering process. It has been widely used to test how well the few-nucleon systems can be described in terms of nucleon-nucleon (NN) interactions. At energies below the  $\pi$  production threshold ( $E=210$  MeV/u), Faddeev calculations provide rigorous descriptions of the scattering process. During the last several years, polarization observables in  $Nd$  elastic scattering have been studied in a number of experiments at RIKEN [1, 2, 3, 4], KVI [5, 6, 7, 8, 9, 10, 11], IUCF [12, 13, 14] and RCNP [15, 16]. The considerable experimental activities were stimulated, in particular, by the observed discrepancy of  $\sim 30\%$  between differential cross section data [1, 17] measured at energies of 65–135 MeV/nucleon and results of Faddeev calculations [18]. Many of the discrepancies for the differential cross sections and vector analyzing powers at these energies are remedied by the inclusion of the  $2\pi$ -exchange three-nucleon forces (3NFs) such as TM-3NF [19], UrbanaIX-3NF [20] or TM99 [21] into the calculations [22]. But theoretical calculations with 3NFs still have difficulties in reproducing data of some spin observables, for instance, tensor analyzing powers.

At high energies, the forward angle  $Nd$  elastic scattering has been successfully described by the Glauber approach [23]

which takes into account both single and double scattering terms. The interference between the single- and double-scattering amplitudes including the  $D$ - state in the deuteron wave function (DWF) allowed one to explain the filling of the cross section diffractive minimum [24].

At energies 200–600 MeV/nucleon, however, large discrepancies between the experimental data [15, 16, 25, 26] and theoretical predictions in the minimum of the differential cross section are persistent even after inclusion of 3NFs [22, 27]. There are several possible origins for these discrepancies. One is relativistic effects: the relativistic Faddeev approach [28, 29] has been developed for intermediate energies range. It was found that when only NN forces are included in the calculations, the relativistic effects are significant only at backward scattering angles. They are relatively small in the minimum of the differential cross section where the discrepancies between 2N force predictions and data are largest [28]. The extension of the Faddeev calculation technique into the relativistic regime [30, 31] also does not provide a reasonable description of the experimental data, only with NN forces. Recently, however, it is reported that large changes of the elastic scattering cross section in the region of angles ranging from the minimum of the cross section up to very backward angles are observed when 3NFs are included in the calculations [29].

Another possibility is the manifestation of new 3NFs. Existing 3NF models [19, 20, 21] mostly deal with low-momentum diagrams, while diagrams with higher momentum can make visible contributions in scatterings at 200–600 MeV/nucleon where large momentum transfers are relevant. It is also possible to consider reaction mechanisms which are not included in the present Faddeev calculations. In the energy region considered, effects due to  $\pi$  production and on-shell  $\Delta$  excitation are the candidates.

Thus it is strongly anticipated that a reaction theory for the nucleon-deuteron scattering at 200–600 MeV is established and further information on new 3NF is extracted from the scattering data. The energy region lies above the  $\pi$ - production threshold and the applicability of the Faddeev calculation techniques, at least as it is, is not trivial. On the one hand, these energies are not large enough to apply the Glauber approach.

In this work new results on the analyzing powers  $A_y$ ,  $A_{yy}$  and  $A_{xx}$  for  $dp$ - elastic scattering measured at  $T_d^{lab} = 880$  MeV over the c.m. angular range from  $60^\circ$  to  $140^\circ$  are presented and are compared with several theoretical calculations, including Faddeev [18] and Glauber [23] ones.

## 2. Experimental procedure

The experiment has been performed at the Internal Target Station (ITS) [32] at the superconducting synchrotron, Nuclotron at the Laboratory of High Energy Physics, Joint Institute for Nuclear Research. The ITS consists of a spherical scattering chamber and a target sweeping system. The scattering chamber is fixed on the flanges of the Nuclotron ion tube. The disk mounting six different targets is located on the axle of a stepper motor. A target used for the measurement is moved to the center of the ion tube when the particles are accelerated up to the required energy. A  $10 \mu\text{m}$   $\text{CH}_2$  film was used as a proton target. A carbon wire was used to evaluate the background originating from the carbon content in  $\text{CH}_2$ . The signal from the target position monitor [33] was used to tune the accelerator parameters to bring the interaction point close to the center of the ITS chamber. The signals from the monitor were also stored as raw data so that one can use the position information in off-line analysis.

The polarized deuteron beam was provided by the atomic-beam polarized ion source POLARIS [34]. Nuclear polarization is provided via radio-frequency (RF) hyperfine transitions. In this experiment the data were taken for three spin modes: unpolarized, "2-6" and "3-5", which have theoretical maximum polarizations of  $(p_z, p_{zz}) = (0, 0)$ ,  $(1/3, 1)$  and  $(1/3, -1)$ , respectively. Two different RF cells of POLARIS [34] with the working frequencies of 384.9 MHz and 320.1 MHz have been used to provide the "2-6" and "3-5" transitions, respectively. The spin modes were cycled by spill-by-spill. The polarized deuteron beam was accelerated up to  $T_d^{lab} = 880$  MeV by keeping the quantization axis perpendicular to the beam-circulation plane of the Nuclotron. The typical beam intensity in the Nuclotron ring was  $2\text{--}3 \times 10^7$  deuterons per spill with a duration of  $\sim 1$  s, independently on the spin mode.

The detection system was designed for analyzing powers measurements in a wide range of initial deuteron energies [35]. The detector support with mounted 46 plastic scintillation counters was placed downstream the ITS spherical chamber. Each plastic scintillation counter was coupled to a photo-multiplier tube Hamamatsu H7416MOD. Nine proton detectors were installed for left, right and up, but due to space limitation – only four for down directions. The proton detectors were placed at a distance of 600 mm from the target. The angular span of one proton detector was  $2^\circ$  in the laboratory frame, which corresponds to  $\sim 4^\circ$  in the c.m. Four deuteron detectors were placed at scattering angles of deuterons coinciding kinematically with the protons for left, right and up scattering. Only one deuteron detector was used to cover the solid angle corresponding to down scattering. In addition, one pair of detectors was placed to register two protons from quasi-elastic  $pp$ - scattering at  $\theta_{pp} = 90^\circ$  in the c.m. in the horizontal plane to monitor the beam luminosity. The deuteron- and quasi-elastic  $pp$ - detectors were placed at a distance of 560 mm from the target in front of the proton detectors.

The scattered deuterons and recoil protons were detected in kinematical coincidence over the center-of-mass angular range of  $60\text{--}140^\circ$ . The analyzing powers  $A_y$ ,  $A_{yy}$  and  $A_{xx}$  were measured at nine (eight) different angles in the c.m. defined by the position of the proton counters placed in the horizontal (vertical) plane.

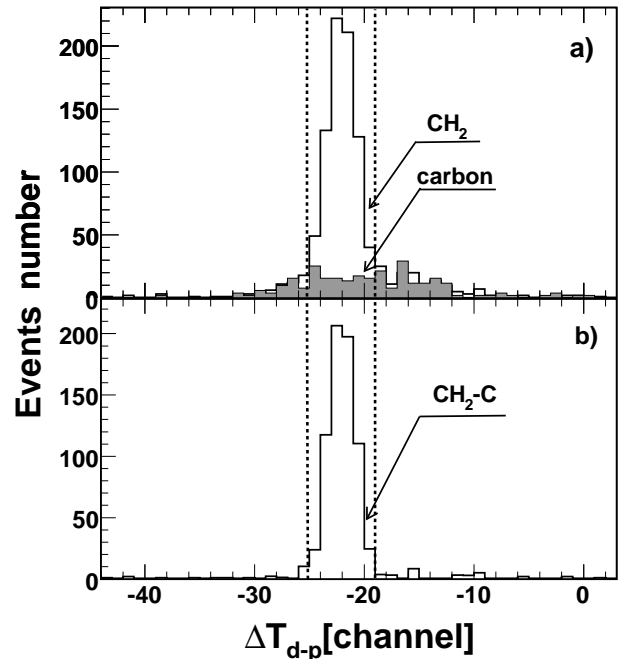


Figure 1: The time difference between the signals for deuteron and proton detectors at  $T_d^{lab} = 880$  MeV and a scattering angle of  $70^\circ$  in the c.m. a) - the normalized spectra obtained for  $\text{CH}_2$  and carbon targets (open and shaded histograms, respectively); b) - the result of the  $\text{CH}_2\text{-C}$  subtraction. The dashed lines are the prompt timing windows to select the  $dp$ - elastic scattering events.

Selection of the  $dp$ - elastic scattering events was based on

the kinematical coincidence of the scattered deuterons and recoil protons by the scintillation counters at several angles in the c.m. The energy loss correlation and time-of-flight difference for the signals from the corresponding proton-deuteron detector pairs were used. The time difference between the signals from the deuteron and proton detectors for CH<sub>2</sub> and carbon targets gated by the correlation on the energy losses are shown in the upper panel in Fig. 1 by the open and shadowed histograms, respectively. The dashed lines in Fig. 1 represent the prompt timing window for the selection of the  $dp$ -elastic scattering events. The carbon contribution is mostly due to quasi-free scattering and appears as a broad bump. It is eliminated partly by the criteria on the energy losses correlation in deuteron and proton scintillation detectors. However, the contribution from the carbon content in CH<sub>2</sub> inside the timing window varied between 10 and 25% depending on the detection angle. The final selection of the  $dp$ -elastic events has been performed by the CH<sub>2</sub>-C subtraction of the normalized time-of-flight difference spectra for each pair of the conjugated deuteron and proton detectors for each spin mode of the PIS [34]. The quality of the CH<sub>2</sub>-C subtraction is demonstrated in the bottom panel in Fig. 1.

The beam polarization has been measured before the data taking using the asymmetry of the  $dp$ -elastic scattering yields at  $T_d^{lab}=270$  MeV with the same detection system [36]. Although the CH<sub>2</sub> film was used as a proton target, no measurements with a carbon target were made, because the background from the carbon content in CH<sub>2</sub> was found negligibly small [35], being in good agreement with RIKEN measurements [1]. Data at several scattering angles were used to decrease the statistical errors of the beam polarization. The values of the analyzing powers  $A_y$ ,  $A_{yy}$ ,  $A_{xx}$  and  $A_{xz}$  at these angles were obtained by the cubic spline interpolation of the precise RIKEN data [3, 37]. The values of the vector  $p_y$  and tensor  $p_{yy}$  components of the beam polarization for the "2-6" and "3-5" spin modes of POLARIS [34] are presented in Table 1. The systematic errors indicated in Table 1 are due to the uncertainty of the  $dp$ -elastic scattering analyzing powers at  $T_d^{lab}=270$  MeV [3, 37].

Table 1: The values of the vector  $p_y$  and tensor  $p_{yy}$  beam polarizations for the "2-6" and "3-5" spin modes of POLARIS [34] obtained at  $T_d^{lab}=270$  MeV [36].

Spin mode	$p_y$	$\Delta p_y^{stat}$	$\Delta p_y^{sys}$	$p_{yy}$	$\Delta p_{yy}^{stat}$	$\Delta p_{yy}^{sys}$
"2-6"	0.216	0.014	0.002	0.605	0.024	0.005
"3-5"	0.208	0.011	0.002	-0.575	0.020	0.005

The analyzing powers  $A_y$ ,  $A_{yy}$  and  $A_{xx}$  for the  $dp$ -elastic scattering at  $T_d^{lab}=880$  MeV were measured simultaneously. The analyzing powers are defined in terms of the  $xyz$  coordinate of  $\vec{z}||\vec{k}_i, \vec{y}||\vec{k}_i \times \vec{k}_f$ , and  $\vec{x}||\vec{y} \times \vec{z}$ , where  $\vec{k}_i$  and  $\vec{k}_f$  are the incident and scattered deuteron momenta, respectively. The yields of the  $dp$ -elastic scattering with the vector  $p_z$  and tensor  $p_{zz}$  deuteron polarizations can be written as [38]

$$N_{pol}(\theta, \phi) = N_0(\theta, \phi) \cdot [1 + \frac{3}{2}p_z A_y(\theta) \cos \phi$$

$$+ \frac{1}{2}p_{zz}(A_{yy}(\theta) \cos^2 \phi + A_{xx}(\theta) \sin^2 \phi)], \quad (1)$$

where  $N_{pol}(\theta, \phi)$  and  $N_0(\theta, \phi)$  are the yields corrected by the beam luminosity and dead-time with polarized and unpolarized beams, respectively,  $\theta$  is the scattering angle, and  $\phi$  is the azimuthal angle with respect to the beam direction. The azimuthal angles  $\phi$  for the detectors placed in the directions of left, right, up, and down are 0,  $\pi$ ,  $-\pi/2$ , and  $\pi/2$  radians, respectively. The analyzing powers  $A_y$ ,  $A_{yy}$  and  $A_{xx}$  were extracted by using the normalized yields  $n(\theta, \phi) = N_{pol}(\theta, \phi)/N_0(\theta, \phi)$ , defined in Eq. (1)

$$\begin{aligned} A_y(\theta) &= \frac{n(\theta, 0) - n(\theta, \pi)}{3p_z} \\ A_{yy}(\theta) &= \frac{n(\theta, 0) + n(\theta, \pi) - 2}{p_{zz}} \\ A_{xx}(\theta) &= \frac{n(\theta, -\pi/2) + n(\theta, \pi/2) - 2}{p_{zz}}. \end{aligned} \quad (2)$$

Such a method does not require an accurate knowledge of the detector geometries and/or efficiencies of the detection system. The analyzing powers  $A_y$ ,  $A_{yy}$ , and  $A_{xx}$  extracted by Eq. (2) were averaged over "2-5" and "3-6" spin modes of POLARIS [34].

### 3. Results and discussion

The angular dependencies of the vector  $A_y$  and tensor analyzing powers  $A_{yy}$  and  $A_{xx}$  obtained at  $T_d^{lab}=880$  MeV are presented in Fig. 2 by the solid symbols. The error bars are the statistical only. The systematic errors for the vector  $A_y$  and tensor analyzing powers  $A_{yy}$  and  $A_{xx}$  from the uncertainty of the normalization of the beam polarization are  $\sim 7\%$  and  $\sim 4\%$ , respectively. The systematic errors due to the procedure of the  $dp$ -elastic events selection were estimated to be  $\sim 5.5\%$  and  $\sim 2.5\%$  for vector and tensor analyzing powers, respectively.

The solid lines in Fig. 2 are the results of the nonrelativistic Faddeev calculations [22] using the CD-Bonn nucleon-nucleon potential [39]. All partial waves with the total angular momentum of two-nucleon subsystem up to  $j_{max}=5$  were taken into account. One can see that the results of Faddeev calculations based on CD-Bonn potential even without involving 3NFs are in good agreement with all the analyzing powers within the achieved experimental accuracy.

The dashed lines correspond to a relativistic calculation in the multiple scattering expansion formalism [40] up to the second-order terms of the nucleon-nucleon  $t$ -matrix [41] with the use of the CD-Bonn [39] DWF. The parameterization [42] of the  $NN$   $t$ -matrix [41] obtained from the recent phase-shift analysis data SP07 [43] allows to avoid the convergence problem due to maximal number of partial wave states in the  $NN$  system. The model [40] takes into account the off-energy-shell effects. The approach describes reasonably well the angular dependencies of  $A_y$  over the whole angular range of measurements and  $A_{yy}$  at backward angles. It fails to reproduce the behavior of  $A_{xx}$ .

The dot-dashed curves correspond to the relativistic calculation of the optical potential framework [44] up to the total angular momentum  $J = 39/2$ . The results are obtained with the use

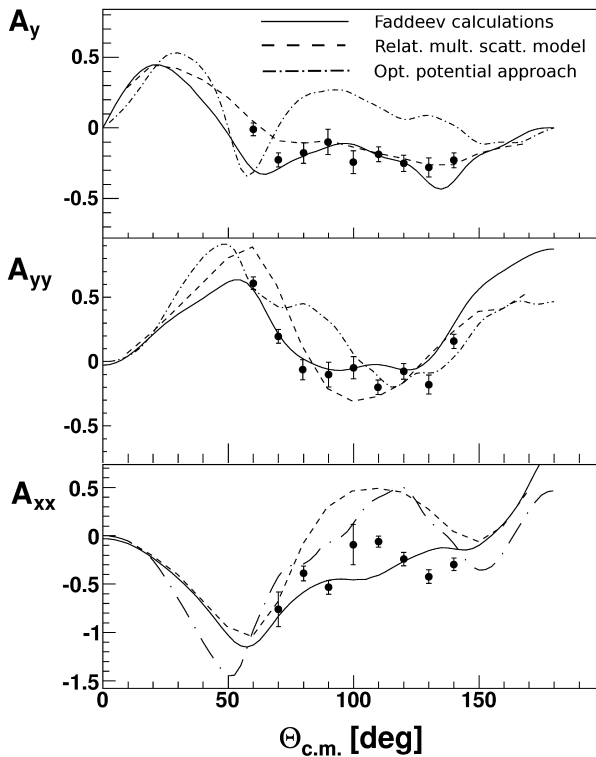


Figure 2: The angular dependencies of the vector  $A_y$  and tensor analyzing powers  $A_{yy}$  and  $A_{xx}$  for  $dp$ -elastic scattering at  $T_d^{lab}=880$  MeV. The lines are explained in the text.

of DWF derived from the dressed bag model of the Moscow-Tübingen group [45] and the on-shell nucleon-nucleon  $t$ -matrix based on the recent phase-shift analysis data SP07 [43]. These calculations reproduce the behavior of  $A_{yy}$  only at the angles larger than  $100^\circ$  in the c.m., while they fail to describe the analyzing powers  $A_y$  and  $A_{xx}$ .

The results of the nonrelativistic Faddeev calculations [22], the relativistic multiple scattering model [40, 46] and the optical potential approach [44] for the  $dp$ -elastic scattering differential cross section at  $T_d^{lab}=880$  MeV are shown in Fig. 3 by the solid, dashed and dash-dotted curves, respectively. They are compared with the experimental data obtained at  $T_d^{lab}=850$  MeV [47] and  $T_d^{lab}=940$  MeV [48] given by the open triangles and circles, respectively.

The optical potential approach [44] which uses the DWF derived from the dressed bag model [45] fails to reproduce the cross section data. Both non-relativistic Faddeev [22] and relativistic multiple scattering [46] calculations describe the experimental data up to the scattering angles in the c.m. of  $\sim 70^\circ$ . The Faddeev approach [22] cannot reproduce the cross section data at larger angles, while the relativistic multiple scattering model calculations [46] provide better agreement with the data in the vicinity of the differential cross section minimum. Note that the relativistic effects in the framework of Faddeev calculations performed with NN forces are significant only in the region of

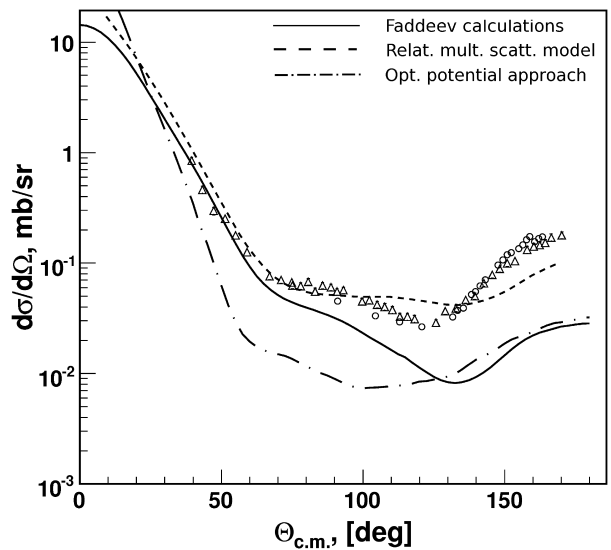


Figure 3: The angular dependence of the  $dp$ -elastic scattering cross section at  $T_d^{lab} \sim 880$  MeV. The solid, dashed and dash-dotted curves are the results of the Faddeev calculation [22], of the relativistic multiple scattering model [40, 46] and of the optical potential approach [44], respectively. The open triangles and circles correspond to the data obtained at  $T_d^{lab}=850$  MeV [47] and  $T_d^{lab}=940$  MeV [48], respectively.

backward angles and they are small in the region of the differential cross section minimum [28]. Therefore, the relativistic effects alone cannot explain the difference between the predictions of these two models. Both approaches cannot reproduce the data at backward scattering angles, where the essential contribution of the  $\Delta$ -isobar excitation into the differential cross section at high energies was demonstrated [49].

The agreement between the cross section data and theoretical calculations at the angles larger than  $70^\circ$  in the c.m. could be improved, if the three-nucleon forces are taken into account. However, theoretical predictions including present 3NF models [20, 21] or an effective 3NF due to explicit  $\Delta$ -isobar excitation [27] underestimate the data at 250 MeV/nucleon [15, 16] by up to 40%. The inclusion of present 3NFs in the calculations does not improve the description of the data on the nucleon analyzing power and proton polarization transfer coefficients obtained at 250 MeV [15, 16]. Therefore, at higher energies, the deviation of both spin observables and cross sections from the theoretical calculations [22, 27, 28] demonstrates the deficiencies of the present 3NF models and relativistic description of the  $dp$ -elastic scattering process. This might indicate that additional short-range 3N forces should be added to the  $2\pi$ -exchange type forces [28, 29].

The relativistic multiple scattering model describes reasonably well the  $dp$ -elastic scattering differential cross section and vector analyzing power  $A_y$  up to  $140^\circ$  in the c.m. [40, 46]. However, it reproduces the behavior of the tensor analyzing power  $A_{yy}$  only at backward angles, while the angular dependence of  $A_{xx}$  is not described. The agreement between the experimental

data and theoretical description could be improved, if the 3NF are included into consideration.

#### 4. Conclusions

The vector  $A_y$  and tensor analyzing powers  $A_{yy}$  and  $A_{xx}$  for  $dp$ - elastic scattering have been measured for the first time at Internal Target Station at the JINR Nuclotron at  $T_d^{lab}=880$  MeV over the c.m. angular range from  $60^\circ$  to  $140^\circ$  corresponding to the transverse momenta of  $\sim 400$ - $600$  MeV/ $c$ .

New results on the tensor analyzing powers indicate strong deviations from the predictions of the relativistic phenomenological approaches [40, 44] based on the use of the nucleon-nucleon forces only. The non-relativistic Faddeev calculations [22] using CD-Bonn 2NF [39] describe only the angular behavior of the new data for the analyzing powers. They, however, fail to reproduce the differential cross section data obtained in earlier experiments [47, 48].

Some deficiencies in the description of the differential cross section and the deuteron analyzing powers at  $T_d^{lab} \sim 880$  MeV obtained at quite large transverse momenta require the consideration of additional mechanisms, for instance, 3NFs. Since present 3NFs models cannot improve the agreement with the data obtained at lower energies [15, 16], new models of 3NFs (including short-range part) should be considered.

The authors are grateful to the Nuclotron accelerator and POLARIS groups. They thank L.S. Azhgirey, Yu.S. Anisimov, E. Ayush, A.F. Elishev, V.I. Ivanov, L.V. Karnjushina, J. Kliman, Z.P. Kuznezova, A.P. Laricheva, A.G. Litvinenko, V. Matousek, M. Morhach, V.G. Perevozchikov, V.M. Slepnev, I. Turzo, Yu.V. Zanevsky and V.N. Zhmyrov for their help during the preparation and performance of the experiment. The investigation has been partly supported by the Grant-in-Aid for Scientific Research (Grant No. 14740151) of the Ministry of Education, Culture, Sports, Science, and Technology of Japan; by the Russian Foundation for Fundamental Research (Grant No. 10-02-00087-a); and by the Polish National Science Center as research project No. DEC-2011/01/B/ST2/00578. Part of the numerical calculations were performed on the supercomputer cluster of the JSC, Jülich, Germany.

#### References

[1] N. Sakamoto et al., Phys.Lett. B367 (1996) 60.  
 [2] H. Sakai et al., Phys.Rev.Lett. 84 (2000) 5288.  
 [3] K. Sekiguchi et al., Phys.Rev. C65(2002) 034003.  
 [4] K. Sekiguchi et al., Phys.Rev. C70 (2004) 014001.  
 [5] R. Bieber et al., Phys. Rev. Lett. 84 (2000) 606.  
 [6] K. Ermisch et al., Phys. Rev. Lett. 86 (2001) 5862.  
 [7] K. Ermisch et al., Phys. Rev. C71 (2005) 064004.  
 [8] E. Stephan et al., Phys.Rev. C76 (2007) 057001.  
 [9] H. Mardanpour et al., Eur.Phys.J. A31 (2007) 383.  
 [10] H.R. Amir-Ahmadi et al., Phys.Rev.C75 (2007) 041001(R).  
 [11] A. Ramazani-Moghaddam-Arani et al., Phys.Rev.C78 (2008) 014006.  
 [12] E.J. Stephenson et al., Phys.Rev. C60 (1999) 061001.  
 [13] R.V. Cadman et al., Phys.Rev.Lett. 86 (2001) 967.  
 [14] B.v.Przewoski et al., Phys.Rev. C74 (2006) 064003.  
 [15] K. Hatanaka et al., Phys.Rev.C66 (2002) 044002.

[16] Y. Maeda et al., Phys.Rev.C76 (2007) 014004.  
 [17] H. Shimizu et al., Nucl.Phys. A382 (1982) 242.  
 [18] W. Glöckle, H. Witala, D. Huber, H. Kamada, J. Golak, Phys.Rep. 274 (1996) 107.  
 [19] S. Coon, M. Scadron, P. McNamee, B.R. Barrett, D. Blatt, B. McKellar, Nucl.Phys. A317 (1979) 242.  
 [20] B.S. Pudliner, V.R. Pandharipande, J. Carlson, S.C. Pieper, R.B. Wiringa, Phys.Rev. C56 (1997) 1720.  
 [21] S.A. Coon, H.K. Han, Few-Body Syst. 30 (2001) 131.  
 [22] H. Witala, W. Glöckle, J. Golak, A. Nogga, H. Kamada, R. Skibinski, J. Kuros-Zolnierczuk, Phys. Rev. C63 (2001) 024007.  
 [23] V. Franco, Phys.Rev.Lett. 16 (1966) 944; V. Franco, E. Coleman, Phys.Rev.Lett. 17 (1966) 827.  
 [24] D.R. Harrington, Phys.Rev.Lett. 21 (1968) 1496.  
 [25] K. Ermisch et al., Phys. Rev. C68 (2003) 051001(R).  
 [26] K. Sekiguchi et al., Phys.Rev. C83 (2011) 061001(R).  
 [27] A. Deluva, K. Chmielewski, P.U. Sauer, Phys.Rev. C67 (2003) 034001.  
 [28] H. Witala, W. Glöckle, J. Golak, H. Kamada, Phys. Rev. C71 (2005) 054001.  
 [29] H. Witala, J. Golak, R. Skibiński, W. Glöckle, H. Kamada, W.N. Polyzou, Phys. Rev. C83 (2011) 044001.  
 [30] T. Lin, Ch. Elster, W.N. Polyzou, H. Witala, W. Glöckle, Phys.Rev. C78 (2008) 024002.  
 [31] Ch. Elster, T. Lin, W. Glöckle, S. Jeschonnek, Phys.Rev. C78 (2008) 034002.  
 [32] A.I. Malakhov et al., Nucl.Instrum.Methods in Phys.Res. A440 (2000) 320; Yu.S. Anisimov et al., Proc. of the 7th Int. Workshop on Relativistic Nuclear Physics, 25-30 August 2003, Stara Lesna, Slovak Republic, p.117.  
 [33] Yu.V. Gurchin et al., Phys.Part.Nucl.Lett. 4 (2007) 263.  
 [34] N.G. Anishchenko et al., AIP Conf.Proc. 95 (1983) 445.  
 [35] T. Uesaka et al., Phys.Part.Nucl.Lett. 3 (2006) 305.  
 [36] P.K. Kurilkin et al., Nucl. Instrum. Methods in Phys.Res. A642 (2011) 45.  
 [37] K. Suda et al., Nucl.Instrum. Methods in Phys.Res. A572 (2007) 745.  
 [38] G.G. Ohlsen, Rep.Prog.Phys. 35 (1972) 717.  
 [39] R. Machleidt, Phys. Rev. C63 (2001) 024001.  
 [40] N.B. Ladygina, Phys.Atom.Nucl. 71 (2008) 2039.  
 [41] N.B. Ladygina, e-Print: arXiv:0805.3021 [nucl-th].  
 [42] W.G. Love, M.A. Franey, Phys.Rev. C24 (1981) 1073; 31 (1985) 488.  
 [43] <http://gwdac.phys.gwu.edu>.  
 [44] M.A. Shikhalev, Phys.Atom.Nucl. 72 (2009) 588.  
 [45] V.I. Kukulkin, V.N. Pomerantsev, M. Kaskulov, A. Faessler, J.Phys.G: Nucl.Part.Phys. 30 (2004) 287.  
 [46] N.B. Ladygina, Eur.Phys.J. A42 (2009) 91.  
 [47] N.E. Booth et al., Phys.Rev. D4 (1971) 1261.  
 [48] J.C. Alder et al., Phys. Rev. C6 (1972) 2010.  
 [49] L.P. Kaptari, Few Body Syst. 27 (1999) 189. Phys.Rev. C72 (2005) 054003. W. Glöckle, Phys.Rev. C76 (2007) 014010.